Monitoring water and oxygen splitting at graphene edges and folds: insights into the lubricity of graphitic materials

Paolo Restuccia[a,c], Mauro Ferrario[a], M. C. Righi[a,b,*]

[a] *Dipartimento di Scienze Fisiche, Informatiche e Matematiche, Università di Modena e Reggio Emilia, Via Campi 213/A, 41125 Modena, Italy*
[b] *CNR-Institute of Nanoscience, S3 Center, Via Campi 213/A, 41125 Modena, Italy*
[c] *Department of Chemistry, Imperial College London, 80 Wood Lane, W12 0BZ London, UK*

Abstract

The functionality of graphene as lubricant material is affected by extrinsic factors, such as the film thickness and the environmental conditions. Graphite lubricating capability depends as well on air humidity. To accurately describe the tribochemistry mechanisms underlying these behaviours we adopt a Quantum Mechanics/Molecular Mechanics approach. We show that reactive edges are able to cause a huge friction increase, which is quantified for graphene flakes between sliding diamond surfaces. Moreover, folds spontaneously formed in single layer graphene under tribological conditions are shown to be highly reactive due to carbon re-hybridization. This observation offers a new hint for interpreting the dependence of graphene friction on the number of layers. Both water and oxygen molecules are found to be effective in quenching the reactivity of defects by dissociative chemisorption. However, peculiar mechanisms of water molecules makes humidity more effective than oxygen for enabling the lubricity of graphitic media. They include collective processes as Grotthus-like proton diffusion enhanced by confinement, and the strong change in hydrophilic character of the passivated media. This comprehensive study sheds a new light on debated issues of graphene and graphite tribology, and highlights the potentiality of these materials for metal-free catalysis, e.g., for H production by water splitting.

*Corresponding author
Email address: mcrighi@unimore.it Tel.:+390592055334 (M. C. Righi)

1. Introduction

The massive waste of energy and environmental costs associated to friction and wear has triggered active research activity in the search for novel lubricant materials. Among them 2D materials have recently attracted increasingly attention as environmental-friendly alternative to lubricants additives in base oil [1] and as atomically-thin coatings [2, 3]. Thanks to its mechanical strength [4, 5], and chemical inertness [6] graphene is emerging as an ideal material in this context, as revealed by the extremely low coefficients of friction measured at the nano- and micro-scales [7–14]. However, the tribological performances of graphene as solid lubricant for macroscale contacts are much less impressive, with friction coefficients typically increasing by two orders of magnitudes [15–21], with only few exceptions where lower values have been obtained by realizing a full interfacial coverage by graphene [22, 23]. Furthermore, the effectiveness of graphene as solid lubricant at the macroscale highly depends on the presence of passivating species in the surrounding environment, in particular on air humidity [17, 24–27]. This behaviour is common to graphite, the bulk counterpart of graphene, which has long been used as solid lubricant.

The fact that graphite lubricity is not an intrinsic property of graphite, but depends on the environment, was discovered in the thirties, when it was found that devices lubricated by graphite used in airplanes flying at high altitudes stopped to properly function due to the low humidity conditions [28]. Since then, several experiments have investigated the role of humidity in graphite tribology [29, 30], and different hypotheses have been made. The firstly proposed mechanism assumes that water physisorbed on graphite surface forms a hydration layer that lubricates the contact [31]. Another early considered mechanism is based on the idea that water intercalates between graphite planes increasing their spacing and consequently favours the interlayer slipperiness [32, 33]. Later, it was proposed that the saturation of reactive sites by passivating species present in moist air is the key process for friction reduction [34–38]. However, a validation of this hypothesis through a direct observation of the molecular mechanisms is still lacking and the effects of edges-water interaction on graphene/graphite friction are still debated [39–41].

Monitoring in real-time the processes that occur at the buried sliding interface is, indeed, a crucial challenge not only to discern the effects of humidity in graphitic materials, but also, and more in general, to make decisive progresses in the development of new, effective lubricant materials. Atomistic simulations represent a very powerful tool in this context, especially those based on an *ab initio* approach, which is essential to accurately describe chemical reactions in conditions of enhanced reactivity, as those imposed by the applied mechanical stresses.

In recent years, first principles calculations have been successfully used to study tribochemical mechanisms in different lubricant materials, such as diamond [42–45], layered materials [6, 46–50] and lubricant additives [51–58]. Most of these studies focused on the effect of tribochemical reactions on interfacial adhesion and shear strength, whereas very few studies [43–45, 48, 50, 59] showed how these reactions take place in real time. The yet limited use of *ab initio* Molecular Dynamics (MD) is mainly due to the associated high computational costs, which limit its field of application to system composed of up to few hundred atoms and to simulation times of few tens of ps. In order to overcome these restrictions, classical MD simulations, based on force fields that enable chemical reactions [60, 61], have been widely employed to study tribochemistry processes in recent years [62–72]. However, the refinement of the high number of parameters, e.g., around 90 for the ReaxFF force field, is very cumbersome making it difficult, if not questionable, to extend its application over a wide range of conditions, as needed for tribological processes.

Here we show that significant progress can be made by the possibility, given by the so called Quantum Mechanics/Molecular Mechanics (QM/MM) approach, to combine the computational advantages of classical molecular dynamics with the accuracy of quantum mechanics. In this method, only the system region expected to be chemically active is treated at a full quantum level, while the remaining part is described by classical force fields. QM/MM was developed in 1976 by Warshel and Levitt [73], who then received the Nobel prize in Chemistry for this multiscale approach, and is much used in the simulation of biomolecocular systems [74], while we are not aware of any previous application to tribochemistry. The QM/MM simulations here performed turn out to be of paramount

importance to understand the effects of humidity in graphitic materials, as they provide an accurate description of the collective behavior of confined water molecules that lead to efficient edge passivation. A close comparison with O_2 molecules in similar tribological conditions highlighted the relevance of hydrogen bond networks in favoring the formation of hydrated lubricant media. Together with classical MD simulation of graphene flakes between diamond surfaces, the simulations reported here help uncovering the primary role of edge and fold passivation in enabling graphene/graphite lubricity. Moreover, the high rate of H_2O and O_2 dissociative adsorption that we observed in real time confirms that graphene can have a high potential for gas sensors and novel type of catalysis [75], the phase diagram we provide for graphene edges in presence of different gas molecules may be useful for the research in these contexts. We also analyze the hydrophilicity of the passivated graphene edges.

2. Methods

We consider a prototypical situation, where graphene fragments are sandwiched between two sliding surfaces (here represented by nanoribbons and graphene bilayers, respectively) in the presence of water molecules. A lateral view of the simulation cell is offered in Fig. 1(a). The global system $\boldsymbol{\mathcal{S}}$ is partitioned in two regions: an inner region, $\boldsymbol{\mathcal{I}}$, which is chemically active, described at the quantum level, and an outer region, $\boldsymbol{\mathcal{O}}$, described classically, where chemical reactions are not expected to take place.

The integration of the equations of motion were performed using tools from the LAMMPS package [76] with interactions in the $\boldsymbol{\mathcal{I}}$ region computed quantum mechanically by means of the Quantum Espresso package [77]. The coupling between the two subsystems is realized by a subtractive scheme [74], according to which all the forces among the atoms of the global system $\boldsymbol{\mathcal{S}}$ are derived from the classical force field, separating the contributions restricting the calculation to within the $\boldsymbol{\mathcal{I}}$ region which are then substituted from those that are calculated *ab initio* within the same $\boldsymbol{\mathcal{I}}$ region. The advantage of this approach is the simplicity of the implementation which, in our case, does not require any other assumption to couple the quantum and the classical described regions.

In the QM/MM simulations we use a Perdew-Burke-Ernzerhof (PBE) parametrization [78, 79] as the exchange correlation functional for the treatment of electronic structure. We also correct this term with the semi-empirical Grimme scheme (PBE-D) [80] to take into account the effect of van der Waals interactions. The Brillouin zone is sampled at the Gamma point and we add a gaussian smearing of 0.02 Rydberg to improve the convergence of the calculations and to consider possible metallic states in the systems due to the presence of graphene reactive edges. The energy (density) cut-off for the plane-wave expansion is set to 25 (200) Ry. For the QM/MM calculation with water, the simulation box has 25.7 Å × 29.6 Å × 30.0 Å dimensions, containing 4 graphene layers, 2 graphene ribbons and 24 water molecules, for a total of 1392 atoms, whereas the calculation with oxygen has a 12.8 Å×14.8 Å×30.0 Å simulation cell, containing 2 graphene layers, 1 graphene ribbons and 6 water molecules, for a total of 198 atoms. For both simulations, the same periodic boundary conditions are applied for both the QM and MM regions and the interaction between atoms belonging to the $\mathcal{O}$ region are described by combining the following sets of interactions. The intralayer graphene interaction is modelled by the second generation REBO potential [60, 81], while the interlayer and interaction of graphene with oxygen and hydrogen atoms are modeled by the Lennard-Jones potential with $\varepsilon = 0.055, 0.060, 0.031$ kcal/mol and $\sigma = 3.41, 3.19, 2.81$ Å parameters for the interlayer C-C [82], C-O [83] and C-H [83] interactions respectively. The water and oxygen molecules are fully treated *ab initio*, thus there is no need to include explicit O-O, O-H and H-H interactions in the classical description.

Before starting the simulations, we optimize the geometry of the systems by applying a 11 GPa load, then initial velocities are assigned by sampling randomly the Maxwell distribution at 300 K. The system is initially thermalized at constant temperature $T = 300$ K by means of three separate Nosé-Hoover thermostats (one for the uppermost graphene layers, one for the intercalated region and one for the lowermost graphene layers), with a damping parameter of 33.3 fs. Then, the thermostat of the intercalated region is switched off to let the degrees of freedom of the $\mathcal{I}$ sub-region free to evolve without any temperature control. After thermalization, a shear stress of 1 GPa is applied for the first 5 ps along the $[1\bar{1}00]$ direction of the outermost graphene layers. Finally, the lateral shear stress is removed and

the systems are let free to evolve for 5 ps without any lateral force applied. The total simulation times of the QM/MM simulation is 11 ps, with an integration time step of 10^{-15} s

In the static density functional theory (DFT) calculations for the relative stability of armchair graphene ribbons and their interaction with water and oxygen molecules, a simulation cell of 17.1 Å × 29.6 Å × 19.8 Å dimensions is used. In these calculations, the graphene ribbons are 17.1 Å long and 9.7 Å width, containing a total of 72 carbon atoms. In the calculations concerning the interaction of fully passivated edges, a larger simulation cell of 17.1 Å × 43.2 Å × 19.8 Å is used to accommodate the presence of two fully passivated graphene ribbons. The details for the electronic structure calculations are similar to the QM/MM case, with a energy (density) cut-off for the plane-wave expansion set to 40 (320) Ry, and the Brillouin zone is sampled with a 6×2 (6×1) Monkhorst-Pack grid for the smaller (larger) simulation cell.

The classical MD simulation for the diamond interfaces have been performed using the LAMMPS [76] package with all interactions modelled by the second generation REBO potential [60, 81]. Each diamond slab consisted of a total of 9720 carbon atoms plus 810 terminating hydrogen atoms used to passivate the not-in-contact surface of the diamond slab in order to stabilize it. The low coverage flake monolayer consisted of 14 flakes for a total 384 carbon atoms, plus 180 hydrogen atoms used in the fully passivated case, raising to 720 carbon atoms and 336 hydrogen atoms in the high coverage case. The system was simulated using rectangular periodic boundary conditions in the xy-plane with box lengths equal to $a = 68.293$ Å and $b = 65.715$ Å. In all simulation a normal load of 0.5 GPa was applied by using external forces, orthogonal to the plane, distributed over all the diamond slab atoms. Two Nosé thermostats, with same damping parameter of 33.3 fs, were applied separately to each of the diamond slab to fix the system temperature $T = 300$ K, without affecting the slab peculiar (sliding) velocity.

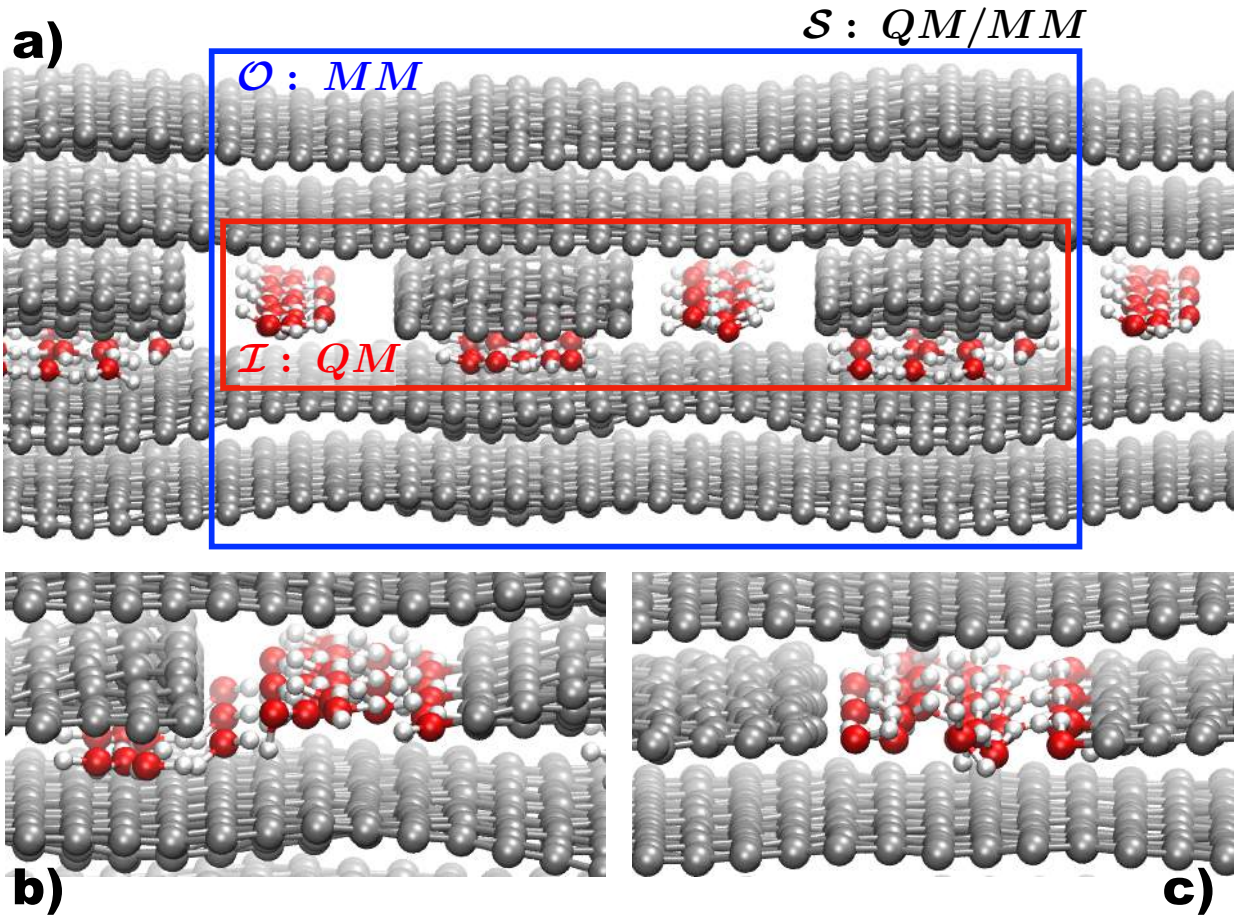

Figure 1: (a) Pictorial representation of the system $\mathcal{S}$ partition: the classical region ($\mathcal{O}$) is represented within blue lines, while the quantum region ($\mathcal{I}$) is detailed by red lines. (b)-(c) Snapshots subsequent in time showing the expulsion of water molecules from the intercalated region below one ribbon, an identical behavior is observed for the other ribbon contained in the supercell. Gray, red and white balls indicate carbon, oxygen and hydrogen atoms, respectively.

3. Results

In spite of the simplicity of the considered model, a series of mechanisms relevant to understand the functionality of graphitic materials emerged during the simulation. They are described and analyzed in the following subsections.

3.1. Water splitting along graphene edges

The first interesting molecular mechanism uncovered by the QM/MM simulation concerns water intercalation. As it can be seen in Figs. 1(b)-(c), the molecules initially positioned between the ribbons and the graphene layer are expelled from the interlayer region and move towards larger interstitial gaps, where reactive sites and other water molecules are present. Water squeezing from the interlayer region, observed during the dynamic simulation, is consistent with the results of DFT calculations performed by our group that predict that in the case of an isolated molecule and infinite graphene layers, intercalation is less energetically favorable than physisorption on the basal plane [84]. However, the possibility for water molecules to remain intercalated within graphene flakes depends on the energy balance between the molecule-graphene and graphene-graphene interactions, which is affected by several factors such as the applied load, the number of intercalated molecules, the lateral extension of the graphene flakes and the presence of reactive edges. Thus, it is not surprising that in situations different from those considered here, as for instance in the absence of mechanical stresses applied [85], or the presence of an aqueous environment [86], intercalation has been experimentally observed. While the effects of water intercalation, when present, on graphene friction have not been thoroughly investigated, here we aim at providing insights into the effects of water dissociative chemisorption on graphene hydrofilicity and friction.

The second interesting molecular mechanism uncovered is that water splitting along the graphene edges occurs at very high rate under tribological conditions. In Fig. 2a, the time-evolution of the radial distribution functions (RDF) for the O-H, C-C, C-H and C-O atom pairs is represented. In the present study we consider armchair edges, terminating by a couple of C atoms connected by a triple bond 1.24 Å long. The dissociation of water molecules is dramatically signaled by the decrease in height of the peak, centered around

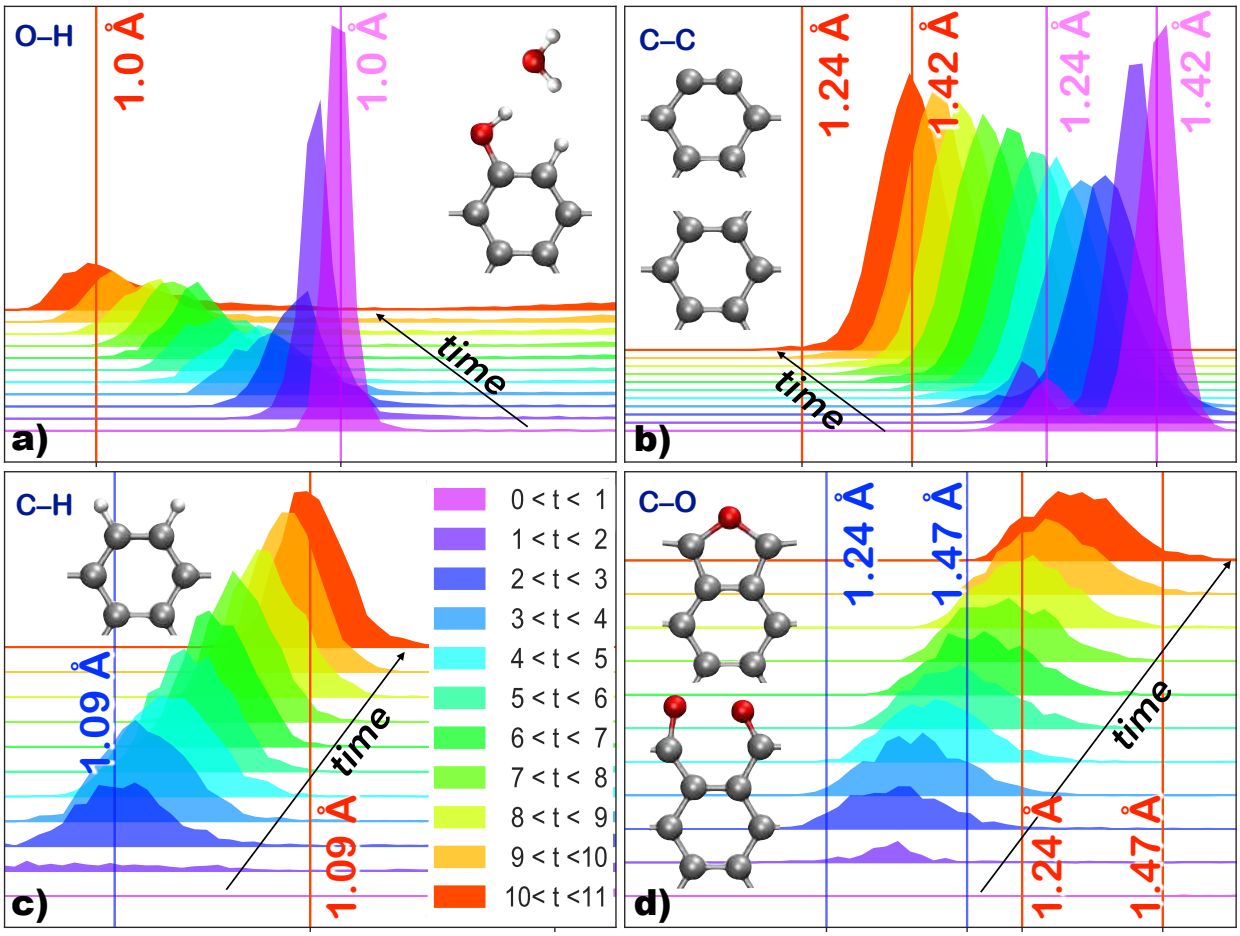

Figure 2: Evolution in time of the short-range atom-atom radial distribution functions calculated over a 1 ps interval. Each panel is labeled according to the atomic pair and shows the most relevant atomic configurations occurring. The same color coded time scale is used for all panels. Curves at different times are uniformly shifted in both, horizontal and vertical, directions, with the same distance scale applied to all panels, corresponding to an interval of 1 Å, with reference bond distances shown as vertical lines, color coded according to the time they are referred to.

0.98 Å, in the O-H RDF and by its subsequent broadening, due to the shorter distance contribution from the chemisorbed O-H groups [Fig. 2(a)]. Correspondingly, one of the two peaks initially present in the C-C RDF disappears after two picoseconds because the C-C triple bonds characteristic of the clean, armchair edges rehybridize into longer, single bonds when passivating species attach to them [Fig. 2(b)]. At the same time, the C-H RDF starts to show a peak around 1 Å, corresponding to the C-H bond length [Fig. 2(c)]. After two picoseconds, a new peak also emerges in the C-O RDF, whose broaden width (from 1.24 Å to 1.47 Å) reflects the larger variety of C-O bonding configurations appearing in the simulations, such as the epoxide, C-O-C, and ketone, C-O, groups shown in Fig. 2(d).

3.2. Grotthus-like proton diffusion enhanced by confinement

The adatom trajectories reported as Movie 1 of the Supplemental Information (SI) reveal that the edge passivation in confined conditions is the result of collective behaviors of water molecules. One remarkable example, illustrated in Figs. 3(a)-(b), is the edge passivation mediated by the formation of hydronium ions. At time t_1 a hydroxyl group of a dissociating water molecule is adsorbed at the edge, while the remaining hydrogen atom is shared by other two water molecules, leading to the formation of H_3O^+ [Fig. 3(a)]. The ion diffuses along the edge, and releases the extra proton after about 0.2 ps [Fig. 3(b)]. Another collective process visible in the QM/MM simulation leads to the formation of an epoxide group: at time t_3 a water molecule promotes the diffusion of a hydrogen atom from a chemisorbed hydroxyl group to a neighbouring oxygen atom [Fig. 3(c)]. The oxygen atom that has lost the hydrogen forms then an epoxide group [Fig. 3(d)]. The full molecular dissociation in C-H and epoxide groups is predicted by DFT as the most energetically favorable dissociative configuration for a water molecule on graphene edges. [84] However, such configuration being the result of collective processes is not observed in a fully-quantum mechanical simulation, based on the Car Parrinello method, of the same duration, but containing a number of atoms reduced by a factor of four with respect to the QM/MM simulation. We performed this simulation, which is presented as Movie 2 in the SI, prior to adopting the QM/MM method. The comparison of the results, while validating the QM/MM approach, allowed

us to identify the importance of cooperative mechanisms in the tribochemistry of graphene interacting with water.

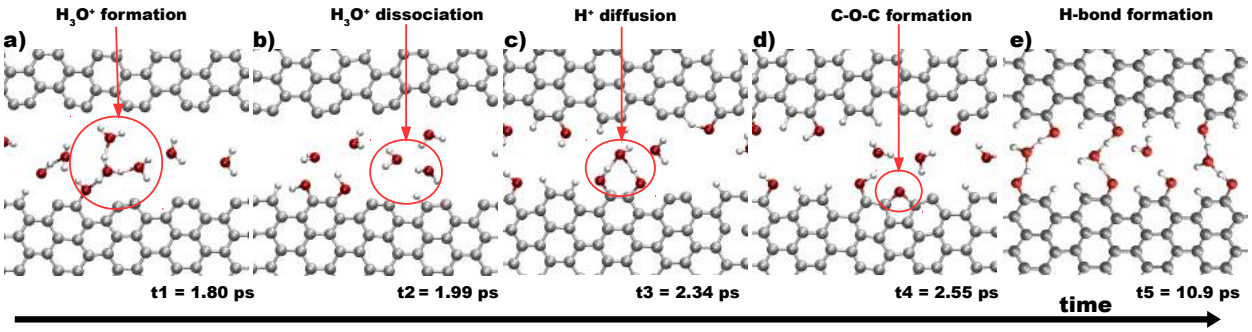

Figure 3: Snapshots, subsequent in time from left to right, showing cooperative mechanisms of water dissociation along graphene edges. (a)-(b) The edge passivation is mediated by the formation and dissociation of a H_3O^+ cation. (c)-(d) The concerted H diffusion along the dimer favors the formation of an epoxide group. (e) Free standing water molecules allow the interaction of fully passivated edges by means of hydrogen bonds.

3.3. Stability of the passivated edges

At the end of the QM/MM simulation almost all the water molecules originally present in the supercell dissociatively adsorb along the graphene edges. The majority of the C-C units become hydrogenated or terminated by water fragments, O termination is observed less frequently. This distribution of the reaction products is in agreement with the stability diagram of the hydrogenated, oxygenated and H_2O-terminated edges represented in Fig. 4.

The diagram is constructed by calculating the formation energy of the passivated edges represented in the picture as a function of the H and O chemical potentials: $E_f = E^p_{tot} - (E^0_{tot} + n_H\mu_H + n_O\mu_O)$, where E^p_{tot} (E^0_{tot}) is the total energy of a passivated (clean) ribbon, n_i is the number of atoms of specie i adsorbed on the edges. Assuming that the chemical potentials (μ_H, μ_O) take values consistent with the presence of hydrogen, oxygen and water molecules [87], one obtains the diagram of Fig. 4, where areas of different color indicate the conditions under which a specific edge termination is found to be the most energetically favorable. We can observe that the clean edge does not appear in the diagram, which means

that clean edges are not expected to survive in the presence of passivating species. The oxygen (hydrogen) termination is expected to prevail only in H-poor (O-poor) atmospheres, while the terminations containing H and OH groups are those expected for a wider ranges of conditions.

3.4. Friction reduction by edge passivation

To make a quantitative assessment of the effects on friction due to edge passivation, as qualitatively highlighted by the previously discussed QM/MM simulations, we have studied the friction arising at the interface of two diamond (111) surfaces when they are separated by small graphene flakes either pristine or hydrogenated. We perform classical MD simulations, allowing us to consider much larger systems, composed of more than 20k atoms, and to follow the dynamics on a longer timescale, of the order of half a nanosecond.

In Fig. 5 we highlight the system atomic structures in the final relaxation stage and compare the observed time behavior for the relative velocity of the two mated surfaces lubricated by pristine graphene flakes and by fully-passivated flakes (aka ovalene and coronene molecules). In the latter case we considered two different amount of flakes, corresponding to 47% and 89% coverage of the surface area. For this particular case, due to the high rigidity of the diamond surfaces, the dynamic friction appears to increase with coverage, modulated mainly by the global size of flake atoms, i.e., proportionally to the effective contact area, at differences with other systems where the work of separation of the interface, and consequently the friction, decreases all the way up to until full coverage is achieved [6].

The behavior of the velocity clearly shows that no sliding occurs in the case of non-passivated flakes as the applied lateral forces are not sufficient to overcome the static friction at the interface, while, when using passivated flakes static friction is greatly reduced and sliding occurs with ease. Dynamical trajectories, included as Movie 3 of the SI, reveal that in both cases the flakes orient themselves parallel to the surfaces. In the absence of passivation the flakes quickly chemically bond with each other and with a few atoms from both the upper and the lower diamond surfaces preventing their relative displacement (only some small-scale oscillatory motion is observed). Passivated flakes on the contrary appears to be

able to move almost freely when between the two surfaces and increasing their number does not modify the overall behavior, the only effect being an increase of friction that can be readily traced to the almost twofold increase of the *contact area*.

3.5. Reactivity of graphene folds and catalytic water splitting on them

In the fully quantum mechanical simulation presented as Movie 2 of SI, a graphene ribbon was sandwiched between two graphene layers, instead of two bilayers as in the QM/MM simulations. This set up, which was chosen to reduce the computational cost of the *ab initio* simulation, reveals that pronounced out-of plane deformations can be formed in single-layer graphene under the effects of mechanical stresses present in tribological contacts (Fig. 6).

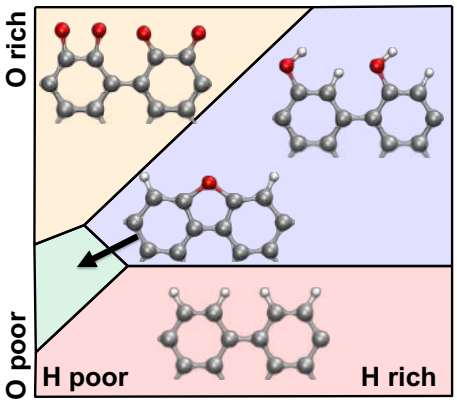

Figure 4: Phase diagram of the graphene armchair edge passivated with hydrogen, oxygen and water. Each domain corresponds to the most stable edge terminations, shown as insets, for the defined values of chemical potential of hydrogen and oxygen.

Moreover, the simulation reveals that the curved graphene regions are very reactive as they can catalyze the dissociation of water molecules. In Fig. 6a the oxygen lone pair is first involved in a bond with a C atoms at the apex of a curved region that has changed its hybridization from sp^2 to sp^3, as revealed the tetrahedral bonding geometry. The intermolecular bonds are weakened until O is completely detached and the H atoms released on the ribbon edges. After an initial metastable configuration, where a keton is observed, the O atom binds to form an epoxy group (Fig. 6b), as often observed in graphene-oxide [88]. The appearance of dangling bonds in the curved region is also evidenced by the formation of

C-C bonds between the atoms belonging to this region and the ribbon edge (Fig. 6b). This results highlight the high reactivity of the curved graphene regions, and the importance of passivating molecules for its reduction by dissociative chemisorption.

3.6. Hydrophilicity of graphitic media where water fragments have been adsorbed

A further outcome of the QM/MM simulations, that we consider worth to analyze in deep, concerns the hydrophilicity of passivated graphene. As highlighted by the atom trajectories reported in Movie 1 of the SI, undissociated water molecules are attracted by passivated edges [Fig. 3(e)]. To quantify the strength of the interaction, we studied water physisorption along the passivated edges previously discussed. The optimized physisorption configurations and energies, reported in Figs. 7(a)-7(d), indicate that all the passivated edges, a part from the hydrogenated one, attract the water molecule more strongly than the clean basal graphene plane, where the physisorption energy is -0.12 eV/molecule [84]. Note that all the calculations include the van der Waals interaction. This result indicates that graphitic media, where water fragments (H, O, and in particular OH) have been adsorbed, became highly hydrophilic. The QM/MM simulation also reveals that these hydrogen-bond networks can interconnect different flakes. An example of this situation is offered in Fig. 3(e), where undissociated molecules assume bridge configurations between passivated edges. This may favors a common orientation of the graphene flakes parallel to the sliding surfaces and the formation of lubricious patches composed of multiple flakes bonded to each other by H bonds.

Comparison with oxygen

The effects of humidity in enabling the lubricity of graphitic media has been reported to be more important than the corresponding effects of oxygen, which is always abundant in air[35, 89]. To investigate the microscopic origin of this observations, we repeat the QM/MM simulation of graphene tribochemistry now considering O_2 molecules instead of the H_2O ones. The adatom trajectories reported in the Movie 4 of the SI show that O_2 molecules initially positioned between the ribbon and the graphene layer remain intercalated until the end of the

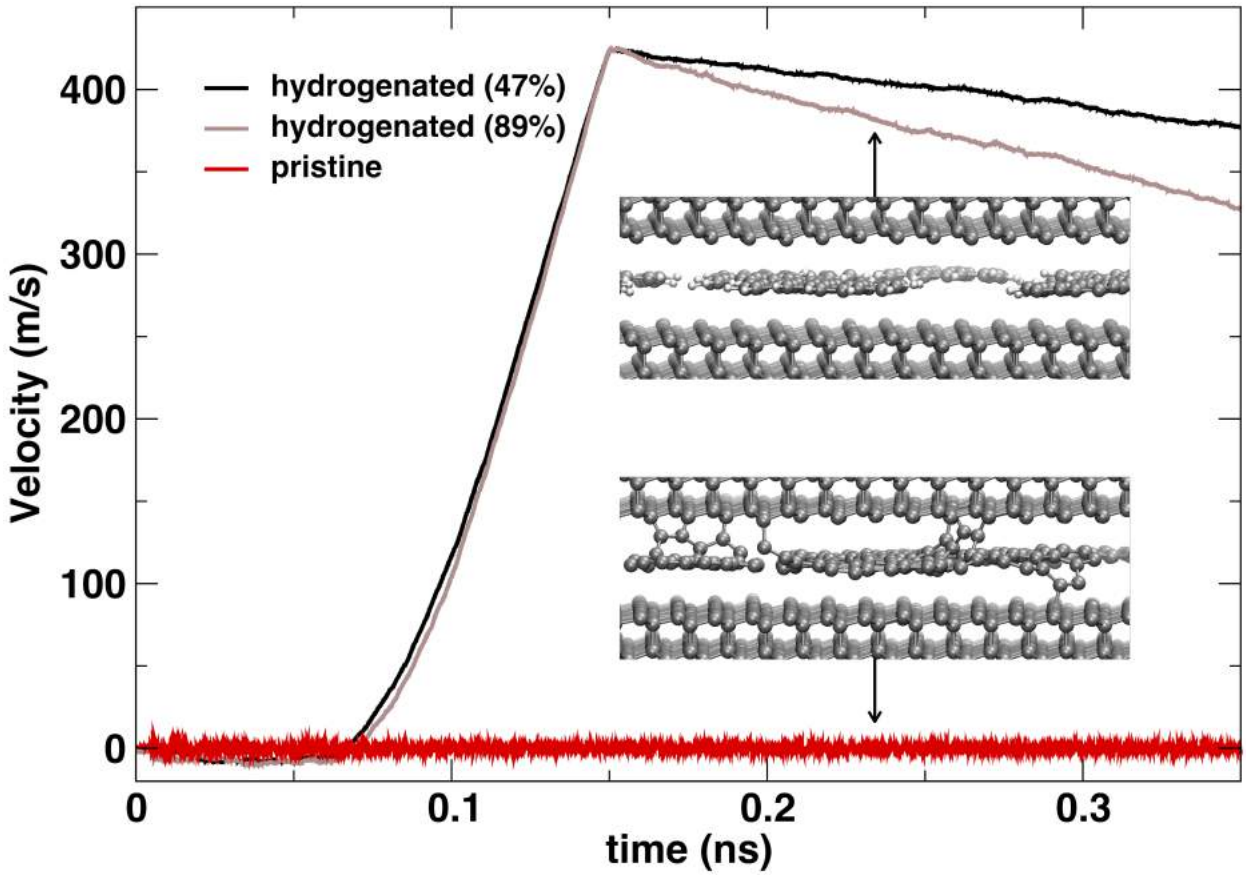

Figure 5: Snapshots of the final atomic configuration for the diamond interface case and the time behavior of the relative diamond slab velocity.

simulation. This behavior is different from the one observed for H_2O molecules and it may be dictated by the stronger physical interaction between the molecule and the graphene basal plane on one hand (the physisorption energy for the O_2 molecule is -0.27 eV/molecule, while for water is -0.12 ev/molecule as mentioned before) and by the weaker molecule-molecule interaction on the other hand. Even if the tendency to intercalate observed in our simulations may be affected by the specific geometry of model, the observed difference between O_2 and H_2O molecules is not coherent with the hypothesis that intercalation increases graphite lubricity.

A second important outcome of the QM/MM simulation carried out for oxygen concerns the chemical reactivity of O_2 molecules, which is shown to be absolutely comparable with that of water molecules. This is confirmed by static DFT calculations that we performed for the sake of comparison, where O_2 molecules positioned in front of graphene edges are observed to spontaneously dissociate as it happens to H_2O molecules [84]. The calculated reaction energies E_R = 7.1 eV and E_R = 6.3 eV calculated for O_2 and H_2O, respectively, reveal that the dissociative chemisorption along the edges is highly exothermic for both the molecules (isolated molecules are considered in the initial states of the reactions). According

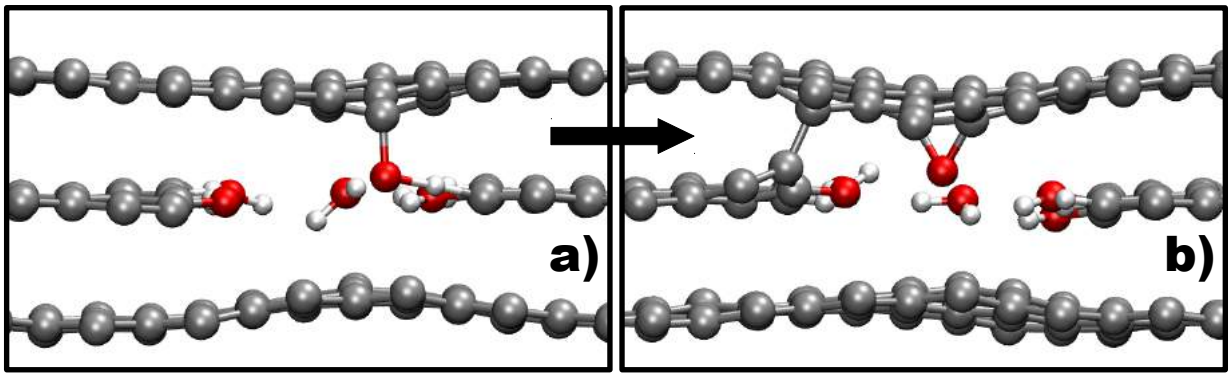

Figure 6: Snapshots subsequent in time acquired during a fully quantum mechanical simulation of single graphene layers interacting with graphene ribbons and water molecules under shear and load. The undulations visible in the graphene structure are due to the applied vertical forces (applied with opposite sign on the top and bottom layers).

to the above outlined analysis neither intercalation nor dissociative chemisorption appear to be the mechanisms that render water vapor more beneficial than oxygen for the lubricity of graphitic materials. We, thus, focus our attention on the property of water molecules to attractively interact, by hydrogen bonds, with chemisorbed water fragments or other molecules physisorbed at the graphitic media. The oxygen gas lacks this property, as evident in Figs. 7e-h, where the result of DFT calculations of O_2 interaction with passivated edges are reported. The O_2 molecules are significantly attracted by the passivated edges only when containing H or OH groups. In the absence of humidity, newly formed edges will be passivated only by oxygen atoms, as revealed by the phase diagram of Fig. 4. Chemisorbed O atoms interact very weakly with other surrounding O_2 molecules (Figs. 7e). Moreover, contrary to what happens for hydroxylated edges, the oxygenated ones are not attracted by each other (Figs. 7i,j). While the effects of edge-edge interaction on the frictional behaviour of graphene/graphite would require further investigation, we nevertheless consider worthy highlight this striking difference between water and oxygen passivation.

4. Discussion

When graphene is used in macroscale applications or subject to severe mechanical stresses it can tear with the consequent exposure of edges.[90] Graphene edges are extremely reactive with estimated formation energies equal to 1.02 and 1.16 eV/Å for armchair and zig-zag edges, respectively [84], thus graphene/graphite flakes with non-passivated edges are anything but lubricious. This is confirmed by the fact that graphite surfaces different from the basal plane are hugely adhesive: the work of adhesion of self-mating (0001) and $(11\bar{2}0)$ surfaces that we calculate here from first principles is equal to 0.24 J/m^2 and to 10.0 J/m^2, respectively. Since adhesive friction increases as power law of the work of adhesion [91, 92], one can expect the friction of graphene/graphite material to change of up to three orders of magnitudes by changing the orientation of graphite crystallites. This is confirmed by the huge friction anisotropy measured experimentally for different surface orientations of graphite [93], and by the increase of friction recorded during atomic friction measurements when scanning across graphene edges [39–41, 94].

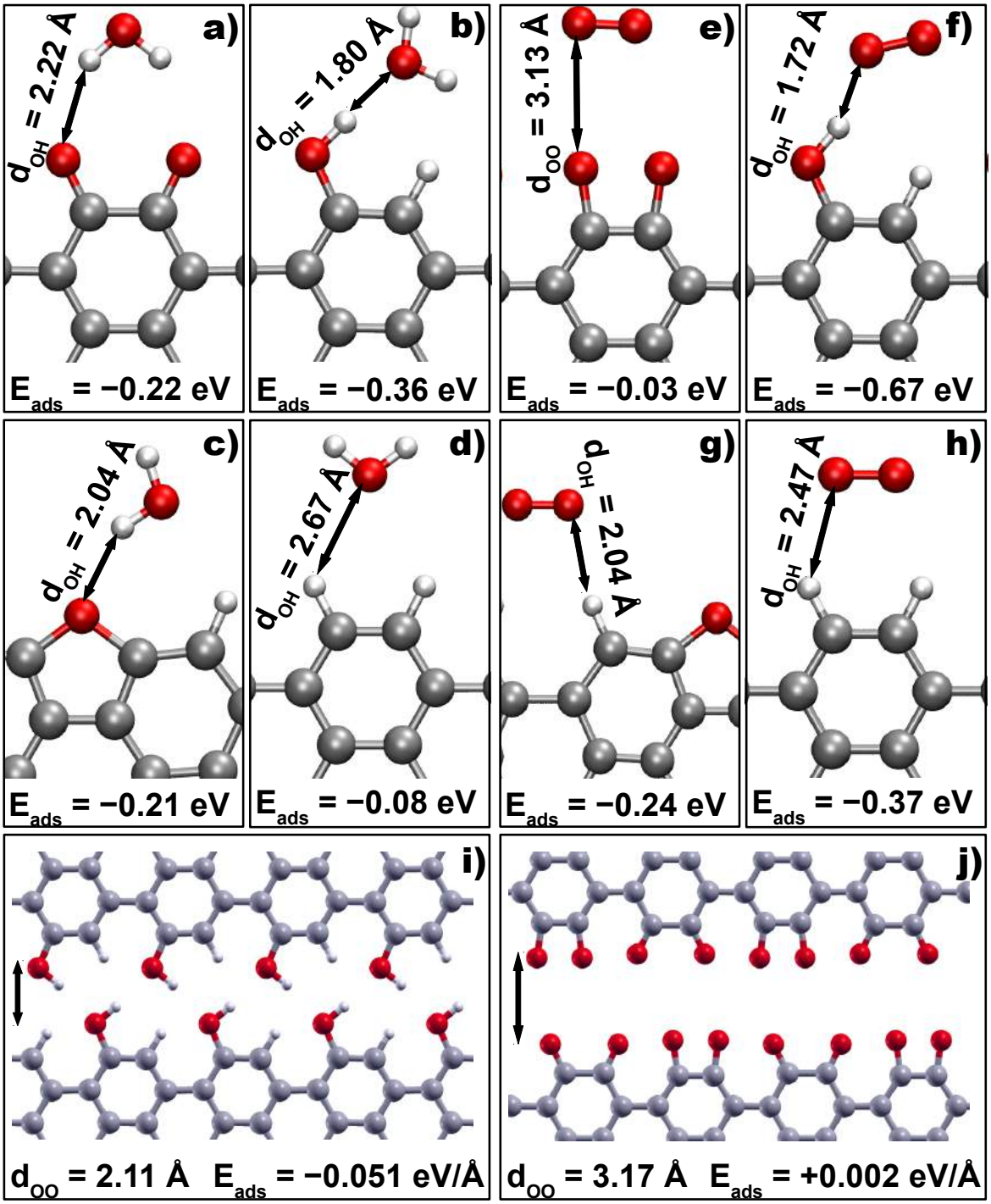

Figure 7: Water (molecular oxygen) adsorption energies and distances for oxygen a) (e), hydroxyl b) (f), epoxide group c) (g) and hydrogen d) (h) terminations are shown, alongside the adhesion energies and distances of fully hydroxilated i) and oxygenated j) graphene ribbons.

It is well know that humidity has a key role in enabling the lubricating capability of graphitic materials. The QM/MM simulations of a tribological interface containing graphene edges and water molecules allows for a direct observation of the fast passivation of the carbon dangling bonds by molecular dissociative chemisorption. This is not only due to the high activation rate of tribochemical reactions, but also to efficient cooperative behaviors of the water molecules confined at the interfaces. An example is provided by the edge hydrogenation promoted by the Grotthus-like proton diffusion, another example is the formation of an epoxide group along the edge as a result of multi-step process. We are able to monitor such processes thanks to the adopted QM/MM approach, as it allows to treat a larger number of molecules than the standard quantum mechanics approach within a computationally affordable simulation time. As demonstrated by the examples described before, collective mechanisms involving critical numbers of water molecules are key in determining the evolution of multi-molecular systems in confined conditions, as those present at solid interfaces. The potentialities of the QM/MM approach for tribology simulations is discussed in a forthcoming article, where the simulations here presented are compared with corresponding fully *ab initio* and classical molecular dynamics simulation [95].

The reaction products observed in the QM/MM are perfectly consistent with the phase diagram that we calculated for armchair edges. The diagram shows, in fact, the thermodynamic instability of clean edges and that the termination containing both H and OH groups is expected for a wider ranges of conditions (taken into account by varying the chemical potentials of the O and H atoms) than either hydrogen- or oxygen-terminations. We are not aware of any previous determination of the relative stability of graphene edge terminations observed in realistic conditions. The experimental characterization of graphene edges is, in fact, extremely challenging, and the terminations considered in previous theoretical phase diagrams are deliberately uncorrelated to their probability to occur [96, 97].

When passivating species are not present, as in vacuum or dry conditions, the tremendously sticky dangling bonds will tend to attach to any surrounding surface. This will completely alter the tribological properties of the graphitic material, especially of graphite that contains a higher density of edges than graphene films, but also of graphene when used

in macroscale applications where new defects can be formed by harsh rubbing.

These observations are confirmed, for larger systems on a longer time scale, by the classical MD simulations of pristine and passivated flakes at the interface between two diamond surfaces. Even relatively small pristine flakes are able to attach simultaneously to both surfaces producing a high static friction, while when only passivated flakes are present the two surfaces can slide with relatively low friction.

Graphene edges or vacancies are not the only reactive sites that can be present in graphitic materials under tribological conditions. An interesting outcome of a fully *ab initio* MD simulation that we performed considering single graphene layers instead of bilayers, reveals, in fact, that the thinner films can undergo much larger out-of-plane deformations under at the effect of mechanical stresses, and that the curved graphene regions are very reactive. We estimate by DFT calculations that the surface energy of graphene increases of 3.96 J/m^2 when a fold is created in a (4x4) unit cell by reducing the cell area by 19%. The C atoms at the convexly curved graphene regions change their hybridization from sp^2 to sp^3 and expose dangling bonds that can interact with edges, forming strong C-C bonds, or catalyze water splitting. This observation is in agreement with the site-selective adsorption of atomic hydrogen on convexly curved regions of monolayer graphene grown on SiC(0001), observed by scanning tunneling microscopy [98].

Out-of plane deformations, or puckers, have been previously introduced to explain the friction enhancement observed in atomic force microscopy experiments when passing from thicker to thinner films of 2D materials [8]. However, the role of puckers in enhancing friction was attributed to an increase of contact area [8, 99, 100]. This explanation was then contradicted by the same authors that had first introduced it: on the basis of classical MD simulations, they showed that the friction increase was substantially larger than the change in contact area due to graphene puckering. Therefore an alternative explanation based on an increase of the contact commensurability was proposed [9]. Here we add a further insight, which is based on the observation that curved graphene is much more adhesive than flat graphene. Out-of-plane deformations are more easily formed in single-layer graphene than on multilayer graphene due to the lower stiffness [101], and the C dangling bonds

appearing at the curved regions can be responsible for the friction enhancement observed in the experiments.

The above discussion highlights the importance of having passivating molecules all around the graphitic media to reduce the reactivity of wrinkles and edges that can be formed during the tribological process. However, it does not provide any specific clue for interpreting the superior effect of humidity on graphite lubricity with respect to other molecular species present in air. Our tribological simulations, where H_2O molecules have replaced the O_2 ones address this issue. The results indicate that oxygen is as efficient as water in passivating the carbon dangling bonds, but it lacks the peculiar property of water molecules to form hydrogen bonds, which can be the key process to interpret the experimental observations. Indeed, the physisorption energies that we calculated with DFT indicate high attraction of water molecules by chemisorbed water fragments. This suggests that the (curved) basal plane, and edges of graphene that have been passivated by water are highly hydrophilic. On the contrary, oxygenated graphene is weakly interacting with surrounding O_2 molecules. Therefore, in humid conditions one can imagine the existence of a reservoir of passivating molecules surrounding the graphitic media able to continuously passivate the reactive sites that are formed during rubbing. Such reservoir of passivating molecules is not expected to be present in dry air. The size of samples that are currently possible to simulate is not large enough to permit quantitative assessments and, in this respect, it would be very useful to have some experimental measure of the increase of oxygen content in the passivated samples correlated with the friction coefficient, in order to understand if there is a passivation threshold below which graphene/graphite does not work as solid lubricant. Moreover, hydrated graphene may be more lubricious than the dry one. It has, in fact, been proposed that a boundary layer of water formed on hydroxylated DLC can be the origin of the very low friction coefficient of this material measured in humid conditions [44]. Moreover, the exfoliation of graphite oxide is more easy than that of graphite[102]. In the specific case of graphene, an hydrated media could favor the flake mobility, making them to more easily reach reactive regions, such as native metallic surfaces, where to adsorb and reduce the interfacial shear strength [20]. On the contrary when a polymer-graphene oxide multilayer

is used, a higher friction coefficient is observed in the presence of humidity with respect to dry air conditions [103, 104]. This appears to be related to the presence of intercalated water molecules that can create hydrogen bonds bridging adjacent layers and so reduce their ability to slide frictionless, as suggested by DFT calculations [104]. If confirmed, one could hypothesize an opposite role of water, with intercalated molecules responsible for an increase of friction and molecules hydrogen bonded to flakes edges reducing friction.

5. Conclusions

In conclusion, the QM/MM method we apply to simulate tribological interfaces allows us both to accurately describe tribochemical reactions and to capture collective processes involving several molecules gathered within the small interfacial space [43, 45]. The simulations reveal that water intercalation does not survive under the effects of the applied load, at variance with what happens for the case of oxygen molecules. Such a difference in the behaviors highly questions the possibility that intercalation plays a primary role in graphite lubricity. The high friction reduction promoted by fully passivated graphene flakes is clearly demonstrated in the classical simulations of diamond interface under sliding, which is, on the contrary, hindered by the presence of sticky pristine flakes. The huge stickiness of graphene edges is further evidenced by calculating their work of adhesion. An extremely high friction anisotropy (up to three orders of magnitudes) is estimated for different graphite crystallite orientations. As shown by our simulations, graphene folds are easily formed in single layer graphene under tribological conditions and they are also common to exfoliated graphite [105]. The high stickiness of the curved graphene regions is quantified by DFT calculations and discussed as possible origin of the increase of friction observed in graphene films by decreasing the number of layers [8]. The key role of passivating species in quenching down the reactivity of edges and faults is highlighted. A close comparison between H_2O and O_2 molecules allows us to identify key mechanisms that can explain the different effect of dry and humid air on the lubricity of graphitic materials. They include concerted behaviors of water molecules, such as hydronium and proton diffusion that are found to promote the fast passivation of graphene edges, and the increase of hydrophilicity caused by water

chemisorption that can result in a hydrated graphitic media more lubricious than the dry one. These results along with the analysis of the thermodynamic stability of hydrogenated, oxygenated and hydroxylated edges, provide useful insights for the application of graphitic materials in tribological, catalytic, and biological applications.

Author contributions

P.R. performed the calculations, analyzed the results, and revised the manuscript. M.F. analyzed the results and revised the manuscript. M.C.R. conducted the project, analyzed the results and wrote the manuscript.

Acknowledgements

The authors thankfully acknowledge M. Ippolito, A. Kohlmeyer and C. Cavazzoni for technical support and CINECA (Consorzio Interuniversitario del Nord est Italiano Per il Calcolo Automatico) for supercomputing resources through the projects Italian SuperComputing Resource Allocation (ISCRA) B TRIBOGMD and TriGMWat. The figures were created with the help of VMD [106] and Matplotlib [107].

Appendix A. Supplementary data

Supplementary data related to this article can be found.

References

[1] H. Xiao, S. Liu, 2D nanomaterials as lubricant additive: A review, Materials & Design 135 (2017) 319 – 332. doi:https://doi.org/10.1016/j.matdes.2017.09.029.
URL http://www.sciencedirect.com/science/article/pii/S0264127517308717

[2] J. C. Spear, B. W. Ewers, J. D. Batteas, 2D-nanomaterials for controlling friction and wear at interfaces, Nano Today 10 (3) (2015) 301 – 314. doi:https://doi.org/10.1016/j.nantod.2015.04.003.
URL http://www.sciencedirect.com/science/article/pii/S174801321500050X

[3] D. Berman, A. Erdemir, A. V. Sumant, Approaches for achieving superlubricity in two-dimensional materials, ACS Nano 12 (3) (2018) 2122–2137. doi:10.1021/acsnano.7b09046.
URL https://pubs.acs.org/doi/10.1021/acsnano.7b09046

[4] K. S. Novoselov, V. I. Fal'ko, L. Colombo, P. R. Gellert, M. G. Schwab, K. Kim, A roadmap for graphene, Nature 490 (2012) 192–200.
URL http://dx.doi.org/10.1038/nature11458

[5] C. Lee, X. Wei, Q. Li, R. Carpick, J. W. Kysar, J. Hone, Elastic and frictional properties of graphene, physica status solidi (b) 246 (11-12) (2009) 2562–2567. doi:10.1002/pssb.200982329.
URL https://onlinelibrary.wiley.com/doi/abs/10.1002/pssb.200982329

[6] P. Restuccia, M. Righi, Tribochemistry of graphene on iron and its possible role in lubrication of steel, Carbon 106 (2016) 118–124. doi:10.1016/j.carbon.2016.05.025.
URL http://www.sciencedirect.com/science/article/pii/S0008622316303797

[7] T. Filleter, J. L. McChesney, A. Bostwick, E. Rotenberg, K. V. Emtsev, T. Seyller, K. Horn, R. Bennewitz, Friction and dissipation in epitaxial graphene films, Phys. Rev. Lett. 102 (2009) 086102. doi:10.1103/PhysRevLett.102.086102.
URL https://link.aps.org/doi/10.1103/PhysRevLett.102.086102

[8] C. Lee, Q. Li, W. Kalb, X.-Z. Liu, H. Berger, R. W. Carpick, J. Hone, Frictional characteristics of atomically thin sheets, Science 328 (5974) (2010) 76–80. doi:10.1126/science.1184167.
URL http://science.sciencemag.org/content/328/5974/76

[9] S. Li, Q. Li, R. W. Carpick, P. Gumbsch, X. Z. Liu, X. Ding, J. Sun, J. Li, The evolving quality of frictional contact with graphene, Nature 539 (2016) 541–545.
URL http://dx.doi.org/10.1038/nature20135

[10] Q. Zheng, B. Jiang, S. Liu, Y. Weng, L. Lu, Q. Xue, J. Zhu, Q. Jiang, S. Wang, L. Peng, Self-retracting motion of graphite microflakes, Phys. Rev. Lett. 100 (2008) 067205. doi:10.1103/PhysRevLett.100.067205.
URL https://link.aps.org/doi/10.1103/PhysRevLett.100.067205

[11] X. Feng, S. Kwon, J. Y. Park, M. Salmeron, Superlubric sliding of graphene nanoflakes on graphene, ACS Nano 7 (2) (2013) 1718–1724. doi:10.1021/nn305722d.
URL https://doi.org/10.1021/nn305722d

[12] S.-W. Liu, H.-P. Wang, Q. Xu, T.-B. Ma, G. Yu, C. Zhang, D. Geng, Z. Yu, S. Zhang, W. Wang, Y.-Z. Hu, H. Wang, J. Luo, Robust microscale superlubricity under high contact pressure enabled by graphene-coated microsphere, Nature Communications 8 (2017) 14029.
URL http://dx.doi.org/10.1038/ncomms14029

[13] Y. J. Shin, R. Stromberg, R. Nay, H. Huang, A. T. Wee, H. Yang, C. S. Bhatia, Frictional characteristics of exfoliated and epitaxial graphene, Carbon 49 (12) (2011) 4070 – 4073. doi:https://doi.org/10.1016/j.carbon.2011.05.046.
URL http://www.sciencedirect.com/science/article/pii/S000862231100409X

[14] D. Marchetto, C. Held, F. Hausen, F. Wählisch, M. Dienwiebel, R. Bennewitz, Friction and wear on single-layer epitaxial graphene in multi-asperity contacts, Tribology Letters 48 (1) (2012) 77–82. doi:10.1007/s11249-012-9945-4.
URL https://doi.org/10.1007/s11249-012-9945-4

[15] K.-S. Kim, H.-J. Lee, C. Lee, S.-K. Lee, H. Jang, J.-H. Ahn, J.-H. Kim, H.-J. Lee, Chemical vapor deposition-grown graphene: The thinnest solid lubricant, ACS Nano 5 (6) (2011) 5107–5114. doi:10.1021/nn2011865.
URL https://doi.org/10.1021/nn2011865

[16] M.-S. Won, O. V. Penkov, D.-E. Kim, Durability and degradation mechanism of graphene coatings deposited on Cu substrates under dry contact sliding, Carbon 54 (2013) 472 – 481. doi:https://doi.org/10.1016/j.carbon.2012.12.007.
URL http://www.sciencedirect.com/science/article/pii/S0008622312009712

[17] D. Berman, S. A. Deshmukh, S. K. R. S. Sankaranarayanan, A. Erdemir, A. V. Sumant, Extraordinary macroscale wear resistance of one atom thick graphene layer, Advanced Functional Materials 24 (42) (2014) 6640–6646. doi:10.1002/adfm.201401755.
URL https://onlinelibrary.wiley.com/doi/abs/10.1002/adfm.201401755

[18] D. Berman, A. Erdemir, A. V. Sumant, Few layer graphene to reduce wear and friction on sliding steel surfaces, Carbon 54 (2013) 454 – 459. doi:https://doi.org/10.1016/j.carbon.2012.11.061.
URL http://www.sciencedirect.com/science/article/pii/S0008622312009529

[19] D. Berman, A. Erdemir, A. V. Sumant, Reduced wear and friction enabled by graphene layers on sliding steel surfaces in dry nitrogen, Carbon 59 (2013) 167 – 175. doi:https://doi.org/10.1016/j.carbon.2013.03.006.
URL http://www.sciencedirect.com/science/article/pii/S0008622313002108

[20] D. Marchetto, P. Restuccia, A. Ballestrazzi, M. Righi, A. Rota, S. Valeri, Surface passivation by graphene in the lubrication of iron: A comparison with bronze, Carbon 116 (2017) 375 – 380. doi:https://doi.org/10.1016/j.carbon.2017.02.011.
URL http://www.sciencedirect.com/science/article/pii/S000862231730129X

[21] J. Ou, J. Wang, S. Liu, B. Mu, J. Ren, H. Wang, S. Yang, Tribology study of reduced graphene oxide sheets on silicon substrate synthesized via covalent assembly, Langmuir 26 (20) (2010) 15830–15836. doi:10.1021/la102862d.
URL https://doi.org/10.1021/la102862d

[22] D. Berman, S. A. Deshmukh, S. K. R. S. Sankaranarayanan, A. Erdemir, A. V. Sumant, Macroscale superlubricity enabled by graphene nanoscroll formation, Science 348 (6239) (2015) 1118–1122. doi:10.1126/science.1262024.

URL http://science.sciencemag.org/content/348/6239/1118

[23] P. Wu, X. Li, C. Zhang, X. Chen, S. Lin, H. Sun, C.-T. Lin, H. Zhu, J. Luo, Self-assembled graphene film as low friction solid lubricant in macroscale contact, ACS Applied Materials & Interfaces 9 (25) (2017) 21554–21562. doi:10.1021/acsami.7b04599.
URL https://doi.org/10.1021/acsami.7b04599

[24] Y. Huang, Q. Yao, Y. Qi, Y. Cheng, H. Wang, Q. Li, Y. Meng, Wear evolution of monolayer graphene at the macroscale, Carbon 115 (2017) 600 – 607. doi:10.1016/j.carbon.2017.01.056.
URL http://www.sciencedirect.com/science/article/pii/S0008622317300660

[25] Z. Li, W. Yang, Y. Wu, S. Wu, Z. Cai, Role of humidity in reducing the friction of graphene layers on textured surfaces, Applied Surface Science 403 (2017) 362 – 370. doi:10.1016/j.apsusc.2017.01.226.
URL http://www.sciencedirect.com/science/article/pii/S0169433217302490

[26] S. Bhowmick, A. Banerji, A. T. Alpas, Role of humidity in reducing sliding friction of multilayered graphene, Carbon 87 (2015) 374 – 384. doi:10.1016/j.carbon.2015.01.053.
URL http://www.sciencedirect.com/science/article/pii/S0008622315000780

[27] Z. Yang, S. Bhowmick, F. G. Sen, A. Banerji, A. T. Alpas, Roles of sliding-induced defects and dissociated water molecules on low friction of graphene, Scientific Reports 8 (1) (2018) 121. doi:10.1038/s41598-017-17971-1.
URL https://www.nature.com/articles/s41598-017-17971-1

[28] E. F. Bracken, Humidity control prevents AC brush disintegration, Electr. World 102 (1933) 410.

[29] J. R. Felts, A. J. Oyer, S. C. Hernández, K. E. Whitener Jr, J. T. Robinson, S. G. Walton, P. E. Sheehan, Direct mechanochemical cleavage of functional groups from graphene, Nature Communications 6 (2015) 6467. doi:10.1038/ncomms7467.
URL https://www.nature.com/articles/ncomms7467

[30] Z. Chen, X. He, C. Xiao, S. H. Kim, Effect of humidity on friction and wear—a critical review, Lubricants 6 (3) (2018) 74. doi:10.3390/lubricants6030074.
URL http://www.mdpi.com/2075-4442/6/3/74

[31] R. H. Savage, Graphite lubrication, Journal of Applied Physics 19 (1) (1948) 1–10. doi:10.1063/1.1697867.
URL https://doi.org/10.1063/1.1697867

[32] G. Rowe, Some observations on the frictional behaviour of boron nitride and of graphite, Wear 3 (4) (1960) 274 – 285. doi:https://doi.org/10.1016/0043-1648(60)90292-1.
URL http://www.sciencedirect.com/science/article/pii/0043164860902921

[33] P. Bryant, P. Gutshall, L. Taylor, A study of mechanisms of graphite friction and wear, Wear 7 (1)

(1964) 118–126. doi:10.1016/0043-1648(64)90083-3.
URL http://www.sciencedirect.com/science/article/pii/0043164864900833?via%3Dihub

[34] J. K. Lancaster, J. R. Pritchard, The influence of environment and pressure on the transition to dusting wear of graphite, Journal of Physics D: Applied Physics 14 (4) (1981) 747.
URL http://stacks.iop.org/0022-3727/14/i=4/a=027

[35] N. Kumar, S. Dash, A. Tyagi, B. Raj, Super low to high friction of turbostratic graphite under various atmospheric test conditions, Tribology International 44 (12) (2011) 1969 – 1978. doi:https://doi.org/10.1016/j.triboint.2011.08.012.
URL http://www.sciencedirect.com/science/article/pii/S0301679X11002313

[36] H. Zaïdi, H. Néry, D. Paulmier, Stability of lubricating properties of graphite by orientation of the crystallites in the presence of water vapour, Applied Surface Science 70-71 (1993) 180 – 185. doi:https://doi.org/10.1016/0169-4332(93)90423-9.
URL http://www.sciencedirect.com/science/article/pii/0169433293904239

[37] J.-C. Rietsch, P. Brender, J. Dentzer, R. Gadiou, L. Vidal, C. Vix-Guterl, Evidence of water chemisorption during graphite friction under moist conditions, Carbon 55 (2013) 90 – 97. doi:https://doi.org/10.1016/j.carbon.2012.12.013.
URL http://www.sciencedirect.com/science/article/pii/S0008622312009803

[38] J. Xiao, L. Zhang, K. Zhou, J. Li, X. Xie, Z. Li, Anisotropic friction behaviour of highly oriented pyrolytic graphite, Carbon 65 (2013) 53 – 62. doi:https://doi.org/10.1016/j.carbon.2013.07.101.
URL http://www.sciencedirect.com/science/article/pii/S0008622313007483

[39] P. Egberts, Z. Ye, X. Z. Liu, Y. Dong, A. Martini, R. W. Carpick, Environmental dependence of atomic-scale friction at graphite surface steps, Phys. Rev. B 88 (2013) 035409. doi:10.1103/PhysRevB.88.035409.
URL https://link.aps.org/doi/10.1103/PhysRevB.88.035409

[40] H. Lang, Y. Peng, X. Zeng, X. Cao, L. Liu, K. Zou, Effect of relative humidity on the frictional properties of graphene at atomic-scale steps, Carbon 137 (2018) 519 – 526. doi:https://doi.org/10.1016/j.carbon.2018.05.069.
URL http://www.sciencedirect.com/science/article/pii/S0008622318305475

[41] Y. Qi, J. Liu, Y. Dong, X.-Q. Feng, Q. Li, Impacts of environments on nanoscale wear behavior of graphene: Edge passivation vs. substrate pinning, Carbon 139 (2018) 59 – 66. doi:https://doi.org/10.1016/j.carbon.2018.06.029.
URL http://www.sciencedirect.com/science/article/pii/S0008622318305852

[42] S. Dag, S. Ciraci, Atomic scale study of superlow friction between hydrogenated diamond surfaces,

Phys. Rev. B 70 (2004) 241401. doi:10.1103/PhysRevB.70.241401.
URL https://link.aps.org/doi/10.1103/PhysRevB.70.241401

[43] G. Zilibotti, S. Corni, M. C. Righi, Load-induced confinement activates diamond lubrication by water, Phys. Rev. Lett. 111 (2013) 146101. doi:10.1103/PhysRevLett.111.146101.
URL http://link.aps.org/doi/10.1103/PhysRevLett.111.146101

[44] S. Kajita, M. C. Righi, A fundamental mechanism for carbon-film lubricity identified by means of ab initio molecular dynamics, Carbon 103 (2016) 193–199. doi:10.1016/j.carbon.2016.02.078.
URL http://www.sciencedirect.com/science/article/pii/S0008622316301713

[45] T. Kuwahara, G. Moras, M. Moseler, Friction regimes of water-lubricated diamond (111): Role of interfacial ether groups and tribo-induced aromatic surface reconstructions, Phys. Rev. Lett. 119 (2017) 096101. doi:10.1103/PhysRevLett.119.096101.
URL https://link.aps.org/doi/10.1103/PhysRevLett.119.096101

[46] L.-F. Wang, T.-B. Ma, Y.-Z. Hu, H. Wang, T.-M. Shao, Ab initio study of the friction mechanism of fluorographene and graphane, The Journal of Physical Chemistry C 117 (24) (2013) 12520–12525. doi:10.1021/jp401097a.
URL http://pubs.acs.org/doi/abs/10.1021/jp401097a

[47] A. Ambrosetti, F. Ancilotto, P. L. Silvestrelli, van der Waals-corrected ab initio study of water ice–graphite interaction, The Journal of Physical Chemistry C 117 (1) (2012) 321–325. doi:10.1021/jp309617f.
URL http://pubs.acs.org/doi/abs/10.1021/jp309617f

[48] T. Onodera, Y. Morita, A. Suzuki, M. Koyama, H. Tsuboi, N. Hatakeyama, A. Endou, H. Takaba, M. Kubo, F. Dassenoy, C. Minfray, L. Joly-Pottuz, J.-M. Martin, A. Miyamoto, A computational chemistry study on friction of h-MoS_2. part i. mechanism of single sheet lubrication, The Journal of Physical Chemistry B 113 (52) (2009) 16526–16536. doi:10.1021/jp9069866.
URL http://pubs.acs.org/doi/abs/10.1021/jp9069866

[49] G. Tocci, L. Joly, A. Michaelides, Friction of water on graphene and hexagonal boron nitride from ab initio methods: very different slippage despite very similar interface structures, Nano Letters 14 (12) (2014) 6872–6877. doi:10.1021/nl502837d.
URL http://pubs.acs.org/doi/abs/10.1021/nl502837d

[50] G. Levita, M. C. Righi, Effects of water intercalation and tribochemistry on MoS_2 lubricity: An ab initio molecular dynamics investigation, ChemPhysChem 18 (11) (2017) 1475–1480. doi:10.1002/cphc.201601143.
URL http://dx.doi.org/10.1002/cphc.201601143

[51] V. Jaiswal, R. B. Rastogi, J. L. Maurya, P. Singh, A. K. Tewari, Quantum chemical calculation

studies for interactions of antiwear lubricant additives with metal surfaces, RSC Advances 4 (26) (2014) 13438–13445. doi:10.1039/C3RA45806G.
URL http://pubs.rsc.org/en/Content/ArticleLanding/2014/RA/c3ra45806g#!divAbstract

[52] D. E. Jiang, E. A. Carter, Carbon atom adsorption on and diffusion into Fe(110) and Fe(100) from first principles, Phys. Rev. B 71 (2005) 045402. doi:10.1103/PhysRevB.71.045402.
URL https://link.aps.org/doi/10.1103/PhysRevB.71.045402

[53] J. M. H. Lo, T. Ziegler, Density functional theory and kinetic studies of methanation on iron surface, The Journal of Physical Chemistry C 111 (29) (2007) 11012–11025. doi:10.1021/jp0722206.
URL http://dx.doi.org/10.1021/jp0722206

[54] D. C. Sorescu, First-principles calculations of the adsorption and hydrogenation reactions of $ch_x(x = 0, 4)$ species on a Fe(100) surface, Phys. Rev. B 73 (2006) 155420. doi:10.1103/PhysRevB.73.155420.
URL https://link.aps.org/doi/10.1103/PhysRevB.73.155420

[55] P. Błoński, A. Kiejna, J. Hafner, Theoretical study of oxygen adsorption at the Fe (110) and (100) surfaces, Surface science 590 (1) (2005) 88–100. doi:10.1016/j.susc.2005.06.011.
URL http://www.sciencedirect.com/science/article/pii/S0039602805006539

[56] N. J. Mosey, M. H. Müser, T. K. Woo, Molecular mechanisms for the functionality of lubricant additives, Science 307 (5715) (2005) 1612–1615. doi:10.1126/science.1107895.
URL http://science.sciencemag.org/content/307/5715/1612

[57] M. Righi, S. Loehlé, M. de Barros Bouchet, D. Philippon, J. Martin, Trimethyl-phosphite dissociative adsorption on iron by combined first-principle calculations and XPS experiments, RSC Advances 5 (122) (2015) 101162–101168. doi:10.1039/C5RA14446A.
URL http://pubs.rsc.org/en/content/articlelanding/2015/ra/c5ra14446a

[58] M. Righi, S. Loehlé, M. D. B. Bouchet, S. Mambingo-Doumbe, J. Martin, A comparative study on the functionality of S- and P-based lubricant additives by combined first principles and experimental analysis, RSC Advances 6 (53) (2016) 47753–47760. doi:10.1039/C6RA07545B.
URL http://pubs.rsc.org/en/content/articlelanding/2016/ra/c6ra07545b

[59] S. Loehlé, M. C. Righi, Ab initio molecular dynamics simulation of tribochemical reactions involving phosphorus additives at sliding iron interfaces, Lubricants 6 (2) (2018) 31. doi:https://doi.org/10.3390/lubricants6020031.
URL http://www.mdpi.com/2075-4442/6/2/31

[60] D. W. Brenner, O. A. Shenderova, J. A. Harrison, S. J. Stuart, B. Ni, S. B. Sinnott, A second-generation reactive empirical bond order (REBO) potential energy expression for hydrocarbons, Journal of Physics: Condensed Matter 14 (4) (2002) 783. doi:10.1088/0953-8984/14/4/312.
URL http://iopscience.iop.org/0953-8984/14/4/312

[61] A. C. T. Van Duin, S. Dasgupta, F. Lorant, W. A. Goddard III, ReaxFF: a reactive force field for hydrocarbons, The Journal of Physical Chemistry A 105 (41) (2001) 9396–9409. doi:10.1021/jp004368u.
URL http://pubs.acs.org/doi/abs/10.1021/jp004368u

[62] B. Bhushan, J. N. Israelachvili, U. Landman, Nanotribology: friction, wear and lubrication at the atomic scale, Nature 374 (6523) (1995) 607–616. doi:10.1038/374607a0.
URL http:https://doi.org/10.1038/374607a0

[63] M. R. Falvo, R. M. Taylor II, A. Helser, V. Chi, F. P. Brooks Jr, S. Washburn, R. Superfine, Nanometre-scale rolling and sliding of carbon nanotubes, Nature 397 (6716) (1999) 236. doi:10.1038/16662.
URL http://www.nature.com/nature/journal/v397/n6716/full/397236a0.html

[64] I. Szlufarska, M. Chandross, R. W. Carpick, Recent advances in single-asperity nanotribology, Journal of Physics D: Applied Physics 41 (12) (2008) 123001.
URL http://stacks.iop.org/0022-3727/41/i=12/a=123001

[65] O. Braun, A. Naumovets, Nanotribology: Microscopic mechanisms of friction, Surface Science Reports 60 (6) (2006) 79–158. doi:10.1016/j.surfrep.2005.10.004.
URL http://www.sciencedirect.com/science/article/pii/S0167572905000853

[66] J. D. Schall, G. Gao, J. A. Harrison, Effects of adhesion and transfer film formation on the tribology of self-mated DLC contacts, The Journal of Physical Chemistry C 114 (12) (2010) 5321–5330. doi:10.1021/jp904871t.
URL http://pubs.acs.org/doi/abs/10.1021/jp904871t

[67] L. Xu, T.-B. Ma, Y.-Z. Hu, H. Wang, Vanishing stick–slip friction in few-layer graphenes: the thickness effect, Nanotechnology 22 (28) (2011) 285708. doi:10.1088/0957-4484/22/28/285708.
URL http://iopscience.iop.org/article/10.1088/0957-4484/22/28/285708/meta

[68] P. Restuccia, M. Ferrario, P. L. Sivestrelli, G. Mistura, M. C. Righi, Size-dependent commensurability and its possible role in determining the frictional behavior of adsorbed systems, Physical Chemistry Chemical Physics 18 (41) (2016) 28997–29004. doi:10.1039/C6CP05386F.
URL http://pubs.rsc.org/en/Content/ArticleLanding/2016/CP/C6CP05386F#!divAbstract

[69] C. Matta, L. Joly-Pottuz, M. I. De Barros Bouchet, J. M. Martin, M. Kano, Q. Zhang, W. A. Goddard III, Superlubricity and tribochemistry of polyhydric alcohols, Phys. Rev. B 78 (2008) 085436. doi:10.1103/PhysRevB.78.085436.
URL https://link.aps.org/doi/10.1103/PhysRevB.78.085436

[70] D.-C. Yue, T.-B. Ma, Y.-Z. Hu, J. Yeon, A. C. van Duin, H. Wang, J. Luo, Tribochemistry of phosphoric acid sheared between quartz surfaces: a reactive molecular dynamics study, The Journal

of Physical Chemistry C 117 (48) (2013) 25604–25614. doi:10.1021/jp406360u.
URL http://pubs.acs.org/doi/abs/10.1021/jp406360u

[71] J. Wen, T. Ma, W. Zhang, G. Psofogiannakis, A. C. van Duin, L. Chen, L. Qian, Y. Hu, X. Lu, Atomic insight into tribochemical wear mechanism of silicon at the Si/SiO_2 interface in aqueous environment: Molecular dynamics simulations using ReaxFF reactive force field, Applied Surface Science 390 (Supplement C) (2016) 216–223. doi:10.1016/j.apsusc.2016.08.082.
URL http://www.sciencedirect.com/science/article/pii/S0169433216317251

[72] J. Yeon, A. C. van Duin, S. H. Kim, Effects of water on tribochemical wear of silicon oxide interface: Molecular dynamics (MD) study with reactive force field (ReaxFF), Langmuir 32 (4) (2016) 1018–1026. doi:10.1021/acs.langmuir.5b04062.
URL http://pubs.acs.org/doi/abs/10.1021/acs.langmuir.5b04062

[73] A. Warshel, M. Levitt, Theoretical studies of enzymic reactions: Dielectric, electrostatic and steric stabilization of the carbonium ion in the reaction of lysozyme, Journal of Molecular Biology 103 (2) (1976) 227 – 249. doi:10.1016/0022-2836(76)90311-9.
URL http://www.sciencedirect.com/science/article/pii/0022283676903119

[74] H. M. Senn, W. Thiel, QM/MM methods for biomolecular systems, Angewandte Chemie International Edition 48 (7) (2009) 1198–1229. doi:10.1002/anie.200802019.
URL http://dx.doi.org/10.1002/anie.200802019

[75] M. Asai, T. Ohba, T. Iwanaga, H. Kanoh, M. Endo, J. Campos-Delgado, M. Terrones, K. Nakai, K. Kaneko, Marked adsorption irreversibility of graphitic nanoribbons for CO_2 and H_2O, Journal of the American Chemical Society 133 (38) (2011) 14880–14883. doi:10.1021/ja205832z.
URL https://doi.org/10.1021/ja205832z

[76] S. Plimpton, Fast parallel algorithms for short-range molecular dynamics, Journal of Computational Physics 117 (1) (1995) 1 – 19. doi:10.1006/jcph.1995.1039.
URL http://www.sciencedirect.com/science/article/pii/S002199918571039X

[77] P. Giannozzi, S. Baroni, N. Bonini, M. Calandra, R. Car, C. Cavazzoni, D. Ceresoli, G. L. Chiarotti, M. Cococcioni, I. Dabo, A. D. Corso, S. de Gironcoli, S. Fabris, G. Fratesi, R. Gebauer, U. Gerstmann, C. Gougoussis, A. Kokalj, M. Lazzeri, L. Martin-Samos, N. Marzari, F. Mauri, R. Mazzarello, S. Paolini, A. Pasquarello, L. Paulatto, C. Sbraccia, S. Scandolo, G. Sclauzero, A. P. Seitsonen, A. Smogunov, P. Umari, R. M. Wentzcovitch, QUANTUM ESPRESSO: a modular and open-source software project for quantum simulations of materials, Journal of Physics: Condensed Matter 21 (39) (2009) 395502. doi:10.1088/0953-8984/21/39/395502.
URL http://iopscience.iop.org/0953-8984/21/39/395502

[78] J. P. Perdew, K. Burke, M. Ernzerhof, Generalized gradient approximation made simple, Phys. Rev.

Lett. 77 (1996) 3865–3868. doi:10.1103/PhysRevLett.77.3865.
URL http://link.aps.org/doi/10.1103/PhysRevLett.77.3865

[79] D. Vanderbilt, Soft self-consistent pseudopotentials in a generalized eigenvalue formalism, Phys. Rev. B 41 (1990) 7892–7895. doi:10.1103/PhysRevB.41.7892.
URL http://link.aps.org/doi/10.1103/PhysRevB.41.7892

[80] S. Grimme, Semiempirical GGA-type density functional constructed with a long-range dispersion correction, Journal of Computational Chemistry 27 (15) (2006) 1787–1799. doi:10.1002/jcc.20495.
URL http://dx.doi.org/10.1002/jcc.20495

[81] S. J. Stuart, A. B. Tutein, J. A. Harrison, A reactive potential for hydrocarbons with intermolecular interactions, The Journal of Chemical Physics 112 (14) (2000) 6472–6486. doi:10.1063/1.481208.
URL http://scitation.aip.org/content/aip/journal/jcp/112/14/10.1063/1.481208

[82] L. A. Girifalco, M. Hodak, R. S. Lee, Carbon nanotubes, buckyballs, ropes, and a universal graphitic potential, Phys. Rev. B 62 (2000) 13104–13110. doi:10.1103/PhysRevB.62.13104.
URL https://link.aps.org/doi/10.1103/PhysRevB.62.13104

[83] R. L. Jaffe, P. Gonnet, T. Werder, J. H. Walther, P. Koumoutsakos, Water–carbon interactions 2: calibration of potentials using contact angle data for different interaction models, Molecular Simulation 30 (4) (2004) 205–216. doi:10.1080/08927020310001659124.
URL http://www.tandfonline.com/doi/full/10.1080/08927020310001659124

[84] G. Levita, P. Restuccia, M. C. Righi, Graphene and MoS_2 interacting with water: a comparison by ab initio calculations, Carbon 107 (2016) 878–884. doi:10.1016/j.carbon.2016.06.072.
URL http://www.sciencedirect.com/science/article/pii/S0008622316305292?via%3Dihub

[85] A. Qadir, Y. W. Sun, W. Liu, P. G. Oppenheimer, Y. Xu, C. J. Humphreys, D. J. Dunstan, Effect of humidity on the interlayer interaction of bilayer graphene, Phys. Rev. B 99 (2019) 045402. doi:10.1103/PhysRevB.99.045402.
URL https://link.aps.org/doi/10.1103/PhysRevB.99.045402

[86] Y. Diao, G. Greenwood, M. C. Wang, S. Nam, R. M. Espinosa-Marzal, Slippery and sticky graphene in water, ACS Nano 13 (2) (2019) 2072–2082. doi:10.1021/acsnano.8b08666.
URL https://doi.org/10.1021/acsnano.8b08666

[87] G. Zilibotti, M. C. Righi, M. Ferrario, Ab initio study on the surface chemistry and nanotribological properties of passivated diamond surfaces, Phys. Rev. B 79 (2009) 075420. doi:10.1103/PhysRevB.79.075420.
URL https://link.aps.org/doi/10.1103/PhysRevB.79.075420

[88] K. A. Mkhoyan, A. W. Contryman, J. Silcox, D. A. Stewart, G. Eda, C. Mattevi, S. Miller, M. Chhowalla, Atomic and electronic structure of graphene-oxide, Nano Letters 9 (3) (2009) 1058–

1063. doi:10.1021/nl8034256.
URL https://pubs.acs.org/doi/10.1021/nl8034256

[89] B. Yen, Influence of water vapor and oxygen on the tribology of carbon materials with sp2 valence configuration, Wear 192 (1) (1996) 208 – 215. doi:https://doi.org/10.1016/0043-1648(95)06807-4.
URL http://www.sciencedirect.com/science/article/pii/0043164895068074

[90] A. Klemenz, L. Pastewka, S. G. Balakrishna, A. Caron, R. Bennewitz, M. Moseler, Atomic scale mechanisms of friction reduction and wear protection by graphene, Nano Letters 14 (12) (2014) 7145–7152. doi:10.1021/nl5037403.
URL https://doi.org/10.1021/nl5037403

[91] M. Wolloch, G. Levita, P. Restuccia, M. C. Righi, Interfacial charge density and its connection to adhesion and frictional forces, Phys. Rev. Lett. 121 (2018) 026804. doi:10.1103/PhysRevLett.121.026804.
URL https://link.aps.org/doi/10.1103/PhysRevLett.121.026804

[92] M. Wolloch, G. Losi, M. Ferrario, M. C. Righi, High throughput screening of the static friction and ideal cleavage strength of solid interfaces, in printing (2019).

[93] J. W. Midgley, D. G. Teer, Surface orientation and friction of graphite, graphitic carbon and non-graphitic carbon, Nature 189 (1961) 735–736. doi:10.1038/189735a0.
URL https://www.nature.com/articles/189735a0

[94] D. P. Hunley, T. J. Flynn, T. Dodson, A. Sundararajan, M. J. Boland, D. R. Strachan, Friction, adhesion, and elasticity of graphene edges, Phys. Rev. B 87 (2013) 035417. doi:10.1103/PhysRevB.87.035417.
URL https://link.aps.org/doi/10.1103/PhysRevB.87.035417

[95] P. Restuccia, M. Ferrario, M. C. Righi, Quantum Mechanics/Molecular Mechanics (QM/MM) applied to tribology: real-time monitoring of tribochemical reactions of water at graphene edges, submitted (2018).

[96] T. Wassmann, A. P. Seitsonen, A. M. Saitta, M. Lazzeri, F. Mauri, Structure, stability, edge states, and aromaticity of graphene ribbons, Phys. Rev. Lett. 101 (2008) 096402. doi:10.1103/PhysRevLett.101.096402.
URL https://link.aps.org/doi/10.1103/PhysRevLett.101.096402

[97] G. J. Soldano, M. F. Juarez, B. W. T. Teo, E. Santos, Structure and stability of graphene edges in O_2 and H_2 environments from ab initio thermodynamics, Carbon 78 (2014) 181 – 189. doi:https://doi.org/10.1016/j.carbon.2014.06.070.
URL http://www.sciencedirect.com/science/article/pii/S0008622314006162

[98] S. Goler, C. Coletti, V. Tozzini, V. Piazza, T. Mashoff, F. Beltram, V. Pellegrini, S. Heun, Influence

of graphene curvature on hydrogen adsorption: Toward hydrogen storage devices, The Journal of Physical Chemistry C 117 (22) (2013) 11506–11513. doi:10.1021/jp4017536.
URL https://doi.org/10.1021/jp4017536

[99] Z. Ye, C. Tang, Y. Dong, A. Martini, Role of wrinkle height in friction variation with number of graphene layers, Journal of Applied Physics 112 (11) (2012) 116102. doi:10.1063/1.4768909.
URL https://doi.org/10.1063/1.4768909

[100] Q. Li, C. Lee, R. W. Carpick, J. Hone, Substrate effect on thickness-dependent friction on graphene, physica status solidi (b) 247 (11-12) (2010) 2909–2914. doi:10.1002/pssb.201000555.
URL https://onlinelibrary.wiley.com/doi/abs/10.1002/pssb.201000555

[101] M. Reguzzoni, A. Fasolino, E. Molinari, M. C. Righi, Friction by shear deformations in multilayer graphene, The Journal of Physical Chemistry C 116 (39) (2012) 21104–21108. doi:10.1021/jp306929g.
URL https://pubs.acs.org/doi/10.1021/jp306929g

[102] M. Cai, D. Thorpe, D. H. Adamson, H. C. Schniepp, Methods of graphite exfoliation, J. Mater. Chem. 22 (2012) 24992–25002. doi:10.1039/C2JM34517J.
URL http://dx.doi.org/10.1039/C2JM34517J

[103] P. Saravanan, R. Selyanchyn, H. Tanaka, S. Fujikawa, S. M. Lyth, J. Sugimura, Ultra-low friction between polymers and graphene oxide multilayers in nitrogen atmosphere, mediated by stable transfer film formation, Carbon 122 (2017) 395 – 403. doi:https://doi.org/10.1016/j.carbon.2017.06.090.
URL http://www.sciencedirect.com/science/article/pii/S0008622317306681

[104] P. Saravanan, R. Selyanchyn, H. Tanaka, D. Darekar, A. Staykov, S. Fujikawa, S. M. Lyth, J. Sugimura, Macroscale superlubricity of multilayer polyethylenimine/graphene oxide coatings in different gas environments, ACS Applied Materials & Interfaces 8 (40) (2016) 27179–27187. doi:10.1021/acsami.6b06779.
URL https://doi.org/10.1021/acsami.6b06779

[105] V. Huc, N. Bendiab, N. Rosman, T. Ebbesen, C. Delacour, V. Bouchiat, Large and flat graphene flakes produced by epoxy bonding and reverse exfoliation of highly oriented pyrolytic graphite, Nanotechnology 19 (45) (2008) 455601. doi:10.1088/0957-4484/19/45/455601.
URL https://doi.org/10.1088%2F0957-4484%2F19%2F45%2F455601

[106] W. Humphrey, A. Dalke, K. Schulten, VMD: Visual molecular dynamics, Journal of Molecular Graphics 14 (1) (1996) 33 – 38. doi:https://doi.org/10.1016/0263-7855(96)00018-5.
URL http://www.sciencedirect.com/science/article/pii/0263785596000185

[107] J. D. Hunter, Matplotlib: A 2D graphics environment, Computing In Science & Engineering 9 (3)

(2007) 90–95. doi:10.1109/MCSE.2007.55.